



Review

Determination of binding constants by affinity chromatography

Donald J. Winzor*

Department of Biochemistry, School of Molecular and Microbial Sciences, University of Queensland, Brisbane, Qld 4072, Australia

Abstract

This review summarizes developments in the use of affinity chromatography to characterize biospecific interactions in terms of reaction stoichiometry and equilibrium constant. In that regard, the biospecificity incorporated into the design of the experiment ensures applicability of the method regardless of the sizes of the reacting solutes. By the adoption of different experimental strategies (column chromatography, simple partition equilibrium, solid-phase immunoassay and biosensor technology protocols) quantitative affinity chromatography can be used to characterize interactions governed by an extremely broad range of binding affinities. In addition, the link between ligand-binding studies and quantitative affinity chromatography is illustrated by means of partition equilibrium studies of glycolytic enzyme interactions with muscle myofibrils, an exercise which emphasizes that the same theoretical expressions apply to naturally occurring examples of affinity chromatography in the cellular environment.

© 2004 Elsevier B.V. All rights reserved.

Keywords: Reviews; Binding constants; Affinity chromatography; Biosensors

Contents

1. Introduction	352
2. Quantitative expressions for evaluating binding constants	352
2.1. Affinity chromatography of a univalent analyte	352
2.2. Equations for a multivalent analyte	353
2.3. Adaptation of the quantitative expressions for column chromatography	353
3. Approaches for evaluating binding constants by quantitative affinity chromatography	354
3.1. Frontal affinity chromatography	354
3.2. Zonal affinity chromatography	356
3.3. Partition equilibrium studies	357
3.4. Radioimmunoassay and enzyme-linked immunosorbent assay techniques	359
3.5. Biosensor technology	360
4. Extension of the approach to high-performance affinity chromatography	362
4.1. Drug interaction with a single class of immobilized affinity sites	362
4.2. Allowance for heterogeneity of immobilized affinity sites	362
4.3. Determination of binding constants from competitive binding experiments	363
4.4. Binding parameters for the drug-albumin interaction in solution	363
5. Interactions of glycolytic enzymes with muscle myofibrils	364
5.1. Interaction of aldolase with the myofibrillar matrix	364
5.2. Myofibrillar interactions of other glycolytic enzymes	365
5.3. Metabolite-effected desorption of aldolase from myofibrils	365
6. Concluding remarks	366
References	366

* Tel.: +61-7-3870-0243; fax: +61-7-3365-4699.

E-mail address: d.winzor@mailbox.uq.edu.au (D.J. Winzor).

1. Introduction

A logical progression from the introduction of affinity chromatography for the purification of solutes [1] was the adaptation of essentially the same principles for quantitative characterization of the interactions governing the procedure [2–4]. Whereas the function of the immobilized ligand in preparative affinity chromatography is simply a selective interaction with a solute of interest, its role in quantitative studies is to provide a means for determining a binding constant for the biospecific interaction. The technique was certainly envisaged initially [2,3] as a column chromatographic procedure in which the matrix was designed to achieve biospecificity of the solute–matrix interaction. However, its adaptation to accommodate the results of partition equilibrium experiments [4,5] has led to the characterization of naturally occurring biphasic interactions such as those between glycolytic enzymes and the muscle myofibrillar matrix [6,7]. Also included within the framework of quantitative affinity chromatography is the determination of equilibrium constants by solid-phase immunoassay procedures [8,9] as well as by biosensor technology [10,11]. Quantitative affinity chromatography has thus become one of the most versatile methods available for characterizing macromolecular interactions. This attribute is extended further in this review than in its predecessors [12–14] by demonstrating the manner in which the results from high-performance affinity chromatography [15] may also be described analytically within the same general framework. Because the basic quantitative expressions are necessarily common to all of these techniques, a brief theoretical section precedes specific consideration of the individual methods.

2. Quantitative expressions for evaluating binding constants

Quantitative affinity chromatography entails the characterization of two equilibria—an interaction of the partitioning solute (analyte, A) with an immobilized affinity ligand (X), and another involving a soluble ligand (S) that interacts either with A or with X (Fig. 1). Both of these situations result in ligand-facilitated elution of analyte from an affinity column. That shown in Fig. 1a is encountered in situations where X is a covalently immobilized form of S [3], whereas the competition between two saccharides for immobilized lectin affinity sites [16] affords an example of the second situation (Fig. 1b).

Although the parameter measured in affinity chromatography is usually an elution volume or the corresponding retention time (elution volume divided by flow rate), the thermodynamic parameter being monitored is a partition coefficient for the distribution of analyte between its soluble and adsorbed states. For this reason, the theoretical expressions tend to be derived on the basis of species concentrations and the law of mass action. These equations

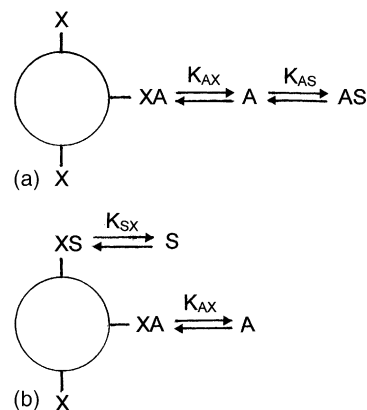


Fig. 1. Schematic representation of the two commonest combinations of interactions encountered in quantitative affinity chromatography. (a) Competition between a soluble ligand (S) and immobilized affinity site (X) for analyte (A). (b) Competition between S and A for immobilized affinity sites X.

are applicable directly to partition equilibrium data and, as will be shown later, are readily adapted to accommodate column chromatographic data, which monitor the analyte distribution by means of elution volume.

2.1. Affinity chromatography of a univalent analyte

For the situation represented in Fig. 1a, the concentration of analyte in the liquid phase, $[\bar{A}]$, is a constitutive parameter that includes a contribution from the concentration of analyte–ligand complex (AS) as well as of free A. Thus,

$$[\bar{A}] = [A] + K_{AS}[A][S] = [A](1 + K_{AS}[S]) \quad (1)$$

where the concentration of analyte–ligand complex has been expressed as the product of the association equilibrium constant (K_{AS}) and the free concentrations of analyte ($[A]$) and competing ligand ($[S]$). The total analyte concentration clearly needs to include A associated with immobilized affinity sites X—a consideration that necessitates the introduction of a doubly constitutive parameter, $[\bar{\bar{A}}]$, such that:

$$[\bar{\bar{A}}] = [A] + K_{AS}[A][S] + K_{AX}[A][X] \quad (2)$$

where the concentration of adsorbed analyte, $[AX]$, is described in terms of the analyte–matrix binding constant (K_{AX}) and the free concentrations of analyte and matrix affinity sites ($[X]$). It then follows that the ratio of analyte concentrations in the solid and liquid phases is defined by the relationship:

$$\frac{[\bar{\bar{A}}] - [\bar{A}]}{[\bar{A}]} = \frac{[\bar{\bar{A}}]}{[\bar{A}]} - 1 = \frac{K_{AX}[X]}{1 + K_{AS}[S]} \quad (3)$$

The concentration of uncomplexed immobilized affinity sites ($[X]$) is not a measurable quantity but can be eliminated by its expression as the difference between the total concentration of immobilized affinity sites ($[\bar{X}]$) and the concentration

of complexed affinity sites, which is also the concentration of adsorbed analyte, $([\bar{A}] - [\bar{A}])$. Thus, Eq. (3) becomes:

$$\frac{[\bar{A}]}{[\bar{A}]} - 1 = \left(\frac{K_{AX}}{1 + K_{AS}[S]} \right) [\bar{X}] - \left(\frac{K_{AX}}{1 + K_{AS}[S]} \right) ([\bar{A}] - [\bar{A}]) \quad (4a)$$

in which K_{AX} , $[\bar{X}]$ and K_{AS} are the parameters to be evaluated by analysis of the distribution data $\{([\bar{A}] - [\bar{A}]), [\bar{A}]\}$. This is the Scatchard [17] linear transform of the rectangular hyperbolic expression:

$$[\bar{A}] - [\bar{A}] = \frac{\{K_{AX}/(1 + K_{AS}[S])\}[\bar{X}][\bar{A}]}{1 + \{K_{AX}/(1 + K_{AS}[S])\}[\bar{A}]} \quad (4b)$$

in situations where a series of experiments is conducted in the presence of a fixed concentration $[S]$ of free ligand. By setting $[S] = 0$ in Eq. (4a) it is immediately evident that K_{AX} and $[\bar{X}]$ are obtained from the slope and intercept, respectively, of the Scatchard plot, $([\bar{A}] - [\bar{A}])/[\bar{A}]$ versus $[\bar{A}] - [\bar{A}]$, of results obtained with a range of analyte concentrations in the absence of competing ligand.

For the other competitive situation (Fig. 1b) the total concentration of analyte in the liquid phase, $[\bar{A}]$, is also its free concentration, $[\bar{A}]$, whereupon the total analyte concentration $[\bar{A}]$ is simply:

$$[\bar{A}] = [\bar{A}] + K_{AX}[\bar{A}][X] \quad (5)$$

However, account needs to be taken of the fact that three species, X, AX and SX, contribute to the total concentration of affinity sites. Consequently, the counterparts of Eqs. (4a) and (4b) become:

$$\frac{[\bar{A}]}{[\bar{A}]} - 1 = \left\{ \frac{K_{AX}}{1 + K_{SX}[S]} \right\} [\bar{X}] - \left\{ \frac{K_{AX}}{1 + K_{SX}[S]} \right\} ([\bar{A}] - [\bar{A}]) \quad (6a)$$

$$[\bar{A}] - [\bar{A}] = \frac{\{K_{AX}/(1 + K_{SX}[S])\}[\bar{X}][\bar{A}]}{1 + \{K_{AX}/(1 + K_{SX}[S])\}[\bar{A}]} \quad (6b)$$

where K_{SX} is the binding constant for the interaction between competing ligand and immobilized affinity sites.

2.2. Equations for a multivalent analyte

For protein analytes exhibiting quaternary structure there is clearly the potential for each analyte subunit to interact with an affinity-matrix site X. Provided that the same intrinsic binding constant [18], K_{AX} , governs all analyte–matrix interactions, the expression analogous to Eqs. (4a) and (4b) for an f -valent analyte in the absence of competing ligand ($[S] = 0$) becomes [19,20]:

$$\left(\frac{[\bar{A}]}{[\bar{A}]} \right)^{1/f} - 1 = K_{AX}[\bar{X}] - fK_{AX}[\bar{A}]^{(f-1)/f} ([\bar{A}]^{1/f} - [\bar{A}]^{1/f}) \quad (7)$$

This expression was derived initially [5,19,20] by means of reacted-site probability theory [21]; but has recently been re-derived [22] by a method bearing much closer similarity to the standard text book approach initiated by Klotz [18] for univalent systems. This latest development in binding theory should engender greater confidence in the validity of Eq. (7) as the counterpart of the Scatchard analysis in situations where the analyte is multivalent.

An obvious prerequisite for the application of Eq. (7) is the assignment of a magnitude to f , the analyte valence. Although some reluctance to make such a decision is understandable, the experimenter must realize that any attempt to avoid the issue by analyzing results in standard Scatchard format merely signifies the selection of unity as the most appropriate number of biospecific sites on the analyte.

2.3. Adaptation of the quantitative expressions for column chromatography

The appearance in Eqs. (4a), (4b) and (7) of terms containing $[\bar{A}]$ and $[\bar{A}]$ dictates the use of frontal chromatography [23] for their rigorous application to experimental data. Frontal chromatography differs from the conventional zonal procedure only in regard to the volume of solution applied to the column. A sufficient sample volume needs to be added to ensure the existence in the elution profile of a plateau region with the composition of the applied solution (Fig. 2). The elution volume (\bar{V}_A) obtained from the median bisector of the analyte boundary (the equivalent position of an infinitely sharp boundary) refers unequivocally to the applied solution with concentration $[\bar{A}]^\alpha$. For a continuously monitored elution profile \bar{V}_A is calculated from the relationship:

$$\bar{V}_A = \left(\frac{1}{[\bar{A}]^\alpha} \right) \sum (V \Delta[\bar{A}]) \quad (8)$$

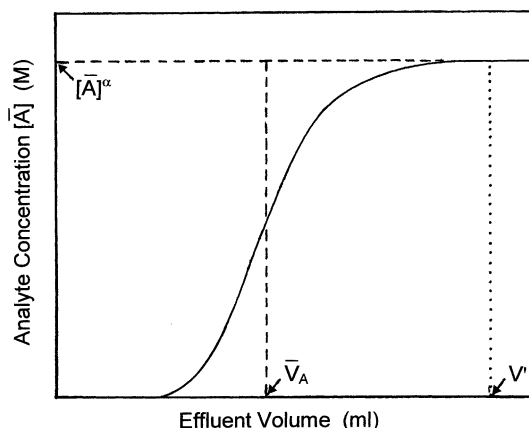


Fig. 2. Schematic representation of the advancing elution profile in frontal chromatography of an analyte solution with applied concentration $[\bar{A}]^\alpha$. The elution volume, \bar{V}_A , obtained as the median bisector of the boundary by means of Eq. (8) or Eq. (9), refers to the applied concentration of analyte, $[\bar{A}]^\alpha$.

where V is the mean effluent volume corresponding to each increment in solute concentration, $\Delta[\bar{A}]$; and where the limits of summation are the solvent plateau ($[\bar{A}] = 0$) preceding the boundary and the plateau of original composition ($[\bar{A}] = [\bar{A}]^\alpha$). In situations where the column effluent is collected as fractions with volume ΔV , a more convenient expression for evaluating the first moment of the boundary is:

$$\bar{V}_A = V' - \left(\frac{1}{[\bar{A}]^\alpha} \right) \sum ([\bar{A}] \Delta V) \quad (9)$$

where $[A]$ is the analyte concentration in a given fraction with volume ΔV , and where V' is the selected upper limit of the summation (Fig. 2). In instances where the boundary is essentially symmetrical, \bar{V}_A is approximated reasonably by the effluent volume at which $[\bar{A}] = [\bar{A}]^\alpha/2$.

The doubly constitutive analyte concentration $[\bar{A}]$ is taken into account by means of a relationship between elution volumes and analyte concentrations that follows from considerations of mass conservation [24]. On the grounds that the product $\bar{V}_A[\bar{A}]$ corresponds to the total amount of solute within the column, this quantity can also be expressed as the product of the volume accessible to analyte, V_A^* , and $[\bar{A}]$. This mass conservation requirement is most conveniently expressed as:

$$\frac{[\bar{A}]}{[\bar{A}]} = \frac{\bar{V}_A}{V_A^*} \quad (10)$$

which allows the direct replacement of the ratio of analyte concentrations by the corresponding ratio of elution volumes. For example, the chromatographic counterpart of Eq. (7) is:

$$\left[\left(\frac{\bar{V}_A}{V_A^*} \right)^{1/f} - 1 \right] = K_{AX}[\bar{X}] - fK_{AX} \left(\frac{\bar{V}_A}{V_A^*} \right)^{(f-1)/f} [\bar{A}] \times \left[\left(\frac{\bar{V}_A}{V_A^*} \right)^{1/f} - 1 \right] \quad (11)$$

The accessible volume, V_A^* , is the elution volume of analyte in the absence of interaction with the affinity matrix—a parameter obtained either as the elution volume in the presence of a saturating concentration of competing ligand or as the elution volume of analyte on an identical column filled with matrix devoid of affinity groups [3,4].

3. Approaches for evaluating binding constants by quantitative affinity chromatography

Because of their development from preparative affinity chromatography, the initial quantitative approaches also entailed the use of column chromatography to characterize the operative equilibria for a particular system. These techniques are therefore considered first.

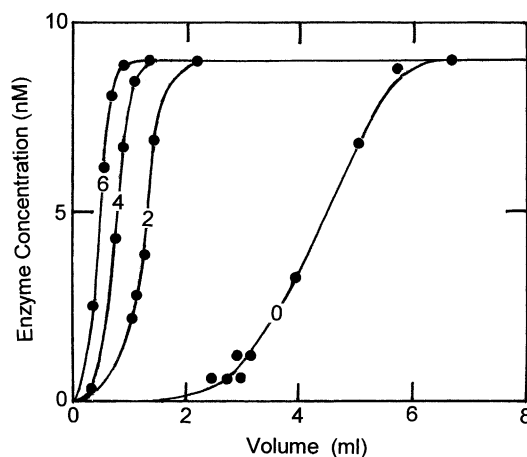


Fig. 3. Elution profiles obtained in frontal chromatography of rat liver lactate dehydrogenase (9 nM) in the presence of the indicated concentrations (μM) of NADH on a 0.1 ml column of 10-carboxydecylamino-Sepharose (data taken from [25]).

3.1. Frontal affinity chromatography

The application of Eq. (11) for the determination of K_{AX} clearly depends upon knowledge of $[\bar{A}]$, the concentration of analyte in the liquid phase. As mentioned in Section 2.3, this is achieved in frontal chromatography by applying analyte solution to the affinity column until the composition of the emerging eluate matches that of the applied solution. Because the affinity column can be small, this requirement does not necessarily involve large volumes of analyte solution, even though the applied volume may be many times larger than the column volume. For example, Fig. 3 presents elution profiles from a series of experiments designed to quantify the NADH-facilitated elution of lactate dehydrogenase by frontal chromatography on 10-carboxydecylamino-Sepharose [25]. At least 60 column volumes (6 ml) of applied solution were required to generate the plateau of original composition in the absence of coenzyme. However, the required volume of enzyme NADH mixture decreased progressively with increasing concentration of coenzyme, which competes with matrix affinity sites for the nucleotide-binding domain of the lactate dehydrogenase. In this particular application of frontal affinity chromatography enzymic activity was used as the assay procedure for monitoring analyte concentration ($[\bar{A}]$) in eluate fractions.

Although frontal chromatography was used in the above study, the absence of sufficient data in the absence of NADH precludes the determination of K_{AX} and hence full exploitation of the theory. Attention is therefore turned to another study involving determination of the binding constant for the interaction between NADH and lactate dehydrogenase by frontal affinity chromatography of the enzyme on trinitrophenyl-Sepharose [20]. Mixtures of rabbit muscle lactate dehydrogenase and NADH were prepared by zonal chromatography of concentrated enzyme solution (5 ml,

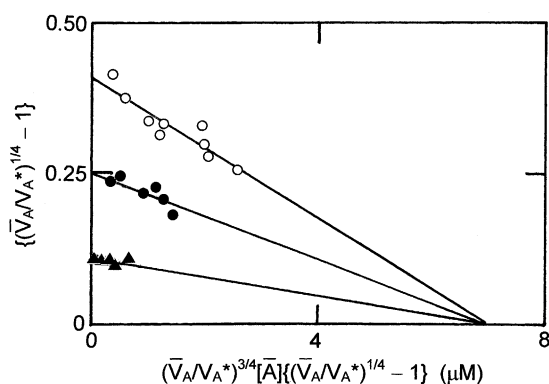


Fig. 4. Analysis of results obtained in frontal chromatography study of the NADH-facilitated elution of rabbit muscle lactate dehydrogenase from a column of trinitrophenyl-Sepharose in terms of Eq. (11) with $f = 4$: data refer to experiments in the absence of coenzyme (O) and to results obtained in the presence of 5 μM (●) and 20 μM (▲) NADH (data taken from [20]).

40 μM) on a column of Sephadex G-25 (2.0 cm \times 21 cm) that had been pre-equilibrated with 0.067 M phosphate buffer (pH 7.2) containing the required free concentration ([S]) of coenzyme (0, 5 or 20 μM). Protein eluted at the void volume was diluted with more of the same buffer-NADH solution to give the required enzyme (analyte) concentration $[\bar{A}]$. The same buffer-NADH solution, which corresponds to the diffusate in equilibrium dialysis [26], was used to pre-equilibrate the column of trinitrophenyl-Sepharose (0.9 cm \times 9.5 cm) to be used for the quantitative characterization.

On the grounds that NADH is a competitive inhibitor of analyte adsorption to the affinity matrix, the lactate dehydrogenase was regarded as being tetravalent ($f = 4$) in order to take into account the existence of a nucleotide-binding domain on each subunit of the tetrameric enzyme. Analysis of the results according to Eq. (11) is summarized in Fig. 4, where the open symbols refer to chromatography of lactate dehydrogenase in the absence of NADH. The essential linearity of this plot signifies that interactions between sites on the enzyme and the affinity matrix are described adequately by a single binding constant (K_{AX}) of $1.5 \times 10^4 \text{ M}^{-1}$ and an effective total concentration of immobilized affinity sites ($[\bar{X}]$) of 28 μM . Furthermore, because a constant value of [S] applies to each series of data in the presence of NADH (solid symbols in Fig. 4), these dependencies should also be linear with slope $\bar{K}_{AX} = K_{AX}/(1 + K_{AS}[S])$, where \bar{K}_{AX} is a constitutive binding constant for the analyte–matrix interaction [27]. Although the slopes of the plots reflecting competitive binding of NADH are not as well defined as that of the plot for enzyme alone, advantage can be taken of the obligatory identity of the abscissa intercept, $[\bar{X}]/4$, for all three data sets. A binding constant (K_{AS}) of $1.3 \times 10^5 \text{ M}^{-1}$ for the interaction of NADH with rabbit muscle lactate dehydrogenase is obtained from the dependence of the constitutive binding constant upon NADH concentration.

An alternative approach to the above design of experiment entails the measurement of \bar{V}_A for a series of reaction mixtures with a fixed analyte concentration $[\bar{A}]$ and a range of free ligand concentrations [4,28]. From Eq. (11) the elution volume for analyte concentration $[\bar{A}]$ in the absence of ligand, $(\bar{V}_A)_0$, is given by the relationship:

$$\left[(\bar{V}_A)_0^{1/f} - V_A^{*1/f} \right] = \frac{V_A^{*1/f} K_{AX} [\bar{X}]}{\{1 + fK_{AX}[(\bar{V}_A)_0/V_A^*]^{(f-1)/f} [\bar{A}]\}} \quad (12)$$

whereas, the corresponding expression for the elution volume in the presence of a concentration [S] of free ligand, $(\bar{V}_A)_S$, is:

$$\begin{aligned} (\bar{V}_A)_S^{1/f} - V_A^{*1/f} \\ = \frac{V_A^{*1/f} K_{AX} [\bar{X}]}{1 + K_{AS}[S] + fK_{AX}[(\bar{V}_A)_0/V_A^*]^{(f-1)/f} [\bar{A}]} \end{aligned} \quad (13)$$

Combination of Eqs. (12) and (13) gives rise to the expression:

$$\frac{(\bar{V}_A)_0^{1/f} - (\bar{V}_A)_S^{1/f}}{(\bar{V}_A)_S^{1/f} - V_A^{*1/f}} = \frac{K_{AS}[S]}{1 + fK_{AX}[(\bar{V}_A)_0/V_A^*]^{(f-1)/f} [\bar{A}]} \quad (14)$$

which simplifies to the form

$$\frac{(\bar{V}_A)_0 - (\bar{V}_A)_S}{(\bar{V}_A)_S - V_A^*} = \frac{K_{AS}[S]}{1 + K_{AX}[\bar{A}]} \quad (15)$$

for a univalent analyte [13]. Analysis of data for the other competitive situation (Fig. 1b) merely requires the substitution of K_{SX} for K_{AS} in Eq. (15).

The application of this alternative approach is illustrated by considering the results of a frontal chromatographic study of the competition between glucose and cytochalasin B for immobilized red cell glucose transporter [29]. Analysis of the concentration dependence of the elution volume for cytochalasin B (the analyte A) in terms of Eq. (11) with $f = 1$ yields values of $1.4 \times 10^7 \text{ M}^{-1}$ for K_{AX} and 134 nM for $[\bar{X}]$ (Fig. 5a). Interpretation of the elution volumes $(\bar{V}_A)_S$ for 1 nM cytochalasin B as a function of glucose concentration in terms of Eq. (15) gives an estimate of 29,200 M^{-1} for $K_{SX}/(1 + K_{AX}[\bar{A}])$ from the slope of Fig. 5b, and hence a binding constant of 29,600 M^{-1} for the competing interaction of glucose with immobilized red cell glucose transporter. A comparable value of 26,000 M^{-1} was obtained by analyzing the results according to the relationship:

$$\frac{1}{(\bar{V}_A)_0 - (\bar{V}_A)_S} = \frac{1 + K_{AX}[\bar{A}]}{V_A^* K_{AX} [\bar{X}]} + \frac{(1 + K_{AX}[\bar{A}])^2}{V_A^* K_{AX} K_{SX} [S]} \quad (16)$$

which was an earlier recommended procedure for determining K_{SX} (or K_{AX}) [4,28]. This procedure is inferior to that applied in Fig. 5b inasmuch as the magnitude of $K_{SX}/(1 + K_{AX}[\bar{A}])$ is obtained as the ratio of the ordinate intercept

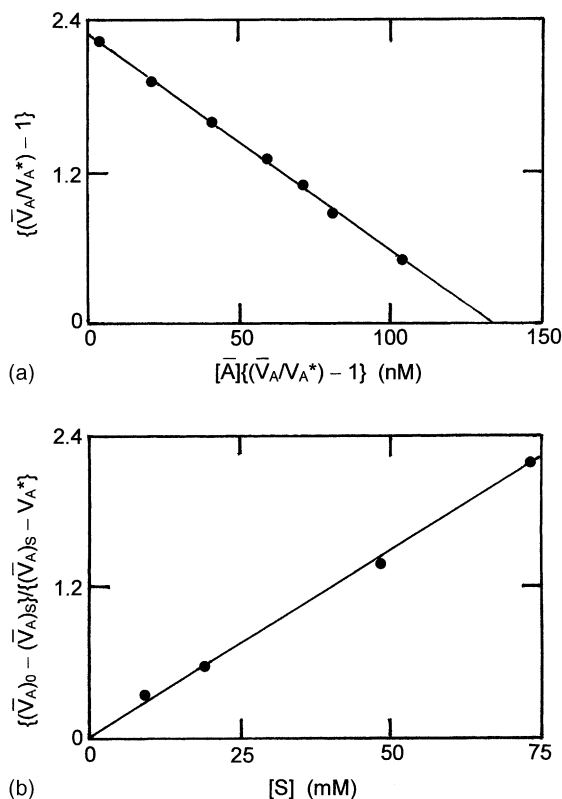


Fig. 5. Characterization of the interaction between glucose and immobilized red cell glucose transporter by a frontal chromatographic study of the glucose-facilitated elution of cytochalasin B. (a) Evaluation of K_{AX} from results obtained in the absence of glucose [Eq. (11) with $f = 1$]. (b) Determination of K_{SX} for the corresponding glucose interaction with immobilized red cell glucose transporter via Eq. (15) (data taken from [29]).

to the slope of the dependence of $1/[(\bar{V}_A)_0 - (\bar{V}_A)_S]$ upon $1/[S]$.

3.2. Zonal affinity chromatography

The measurement of binding constants by the zonal procedure, termed analytical affinity chromatography [30], entails the application of a small zone of analyte solution to a column pre-equilibrated with buffer–ligand mixture and its elution with more of the same buffer–ligand mixture [3]. Although the method enjoys much greater popularity than its frontal counterpart, the dilution that occurs during zonal elution (Fig. 6) precludes the rigorous application of Eq. (11) because of the consequent inability to assign a magnitude to $[\bar{A}]$. It is therefore necessary to neglect the $[\bar{A}]$ term in Eq. (11), which then becomes:

$$(\bar{V}_A/V_A^*)^{1/f} - 1 \approx \left\{ \frac{K_{AX}}{1 + K_{AS}[S]} \right\} [\bar{X}] \quad (17)$$

Use of this truncated form of Eq. (11) entails the assumption that the total concentration of immobilized affinity sites ($[\bar{X}]$) is an adequate estimate of their free concentration ($[X]$)—an approximation that obviously improves with increasing ex-

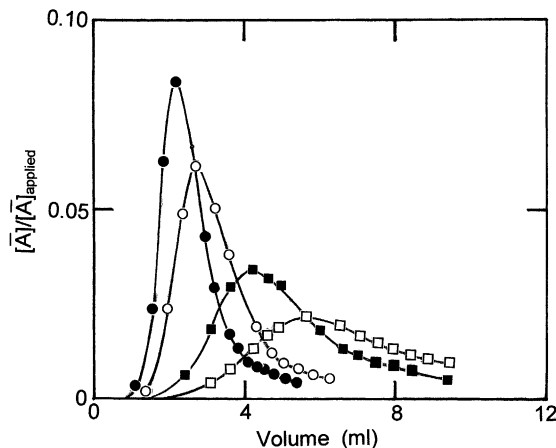


Fig. 6. Elution profiles obtained in zonal chromatography of rat liver lactate dehydrogenase (0.1 ml, 180 nM) on a 10 ml column of 10-carboxydecylamino-Sepharose equilibrated with 8 μ M (\square), 10 μ M (\blacksquare), 15 μ M (\circ) and 18 μ M (\bullet) NADH. Expression of the ordinate scale in terms of the applied enzyme concentration emphasizes the extent of dilution that has occurred during zonal chromatography (data taken from [25]).

tent of affinity site immobilization [20]. Such use of highly substituted affinity matrices was initially considered unsatisfactory for the determination of binding constants [3,31], but that objection reflected the reciprocal linear transform of Eq. (17) being used for a system with $f = 1$, namely,

$$\frac{1}{[\bar{V}_A - V_A^*]} = \frac{V_A^*}{K_{AX}[\bar{X}]} + \frac{V_A^* K_{AS}[S]}{K_{AX}[\bar{X}]} \quad (18)$$

which allows K_{AS} to be determined as the ratio of the slope to the ordinate intercept of the dependence of $1/(\bar{V}_A - V_A^*)$ upon $[S]$ (Fig. 7a). K_{AS} is thus undetermined when the ordinate intercept, $V_A^*/(K_{AX}[\bar{X}])$, becomes indistinguishable from zero because of a large $[\bar{X}]$ value. This difficulty can be avoided [20] by using an alternative linear transform of Eq. (17),

$$\left(\frac{\bar{V}_A}{V_A^*} \right)^{1/f} - 1 = K_{AX}[\bar{X}] - K_{AS}[S] \left\{ \left(\frac{\bar{V}_A}{V_A^*} \right)^{1/f} - 1 \right\} \quad (19)$$

whereupon K_{AS} is obtained directly from the slope ($V_A^* K_{AS}$) of the dependence of $(\bar{V}_A - V_A^*)$ upon $(\bar{V}_A - V_A^*)[S]$ for the system with $f = 1$ (Fig. 7b).

Zonal affinity chromatography thus also affords a reliable means of characterizing ligand binding in situations where the assumed identity of $[X]$ and $[\bar{X}]$ is likely to be a reasonable approximation. In that regard its strength is the ability to yield the analyte elution volume (\bar{V}_A) in an environment with defined free ligand concentration $[S]$ that is used for column pre-equilibration and elution. This feature has rendered possible the simultaneous determination of binding constants for the interaction of NADH with the five isoenzymes of lactate dehydrogenase by zonal affinity chromatography of a crude mouse-tissue extract on oxamate-Sepharose [32], a matrix is selected because of the unique specificity

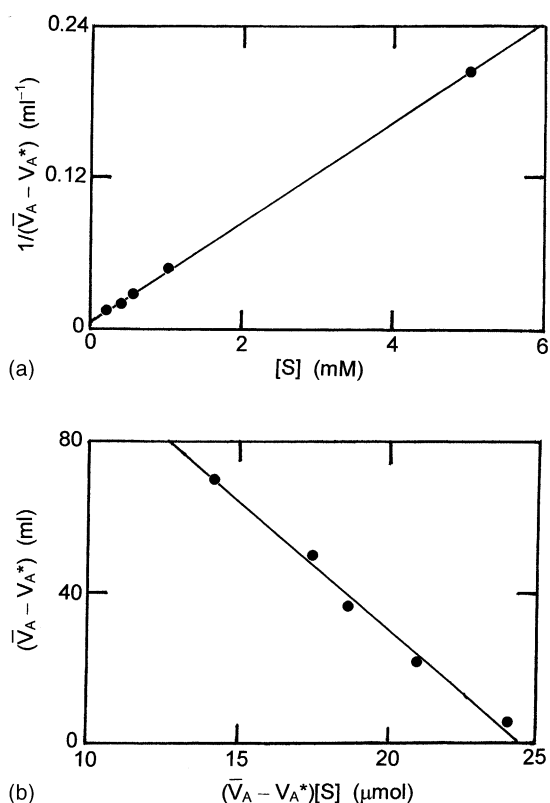


Fig. 7. Characterization of the interaction between *p*-aminobenzamidine and trypsin by zonal affinity chromatography on *p*-aminobenzamidine-Sepharose. (a) Original analysis [31] in terms of Eq. (18). (b) Reanalysis [20] in terms of Eq. (19) (data taken from [31]).

of the immobilized pyruvate analog for binary lactate dehydrogenase complexes. Whereas ligand-facilitated elution of analyte is the usual situation in affinity chromatography, the formation of ternary ASX complex in the above example affords an example of ligand-retarded elution. The retardation of galactosyltransferase from α -lactalbumin-Sepharose by *N*-acetylglucosamine [2] is another example where the biospecific interaction with immobilized affinity sites involves an analyte–ligand complex.

3.3. Partition equilibrium studies

A simple partition equilibrium study entails the preparation of separate mixtures containing known amounts of affinity matrix and analyte, A: some mixtures also contain a known amount (concentration) of competing ligand, S, to allow the evaluation of the second equilibrium constant (K_{AS} or K_{SX}) as well as K_{AX} . After equilibration of the mixtures to establish chemical equilibrium at the temperature of interest, a sample of each supernatant is obtained by filtration [4] or centrifugation [6] at the same temperature. The concentration of analyte in the liquid phase, $[A]$, is then obtained by dividing the amount of added analyte by V_A^* , the volume accessible to analyte. This parameter may be obtained from the distribution of analyte in a mixture containing a suffi-

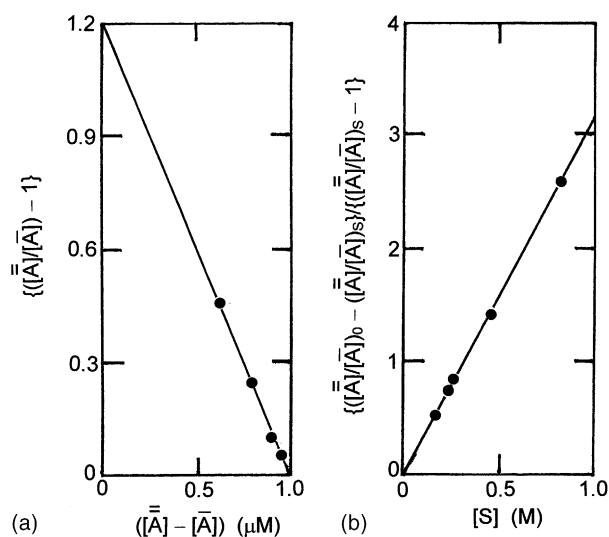


Fig. 8. Characterization of the lysozyme–glucose interaction by means of partition equilibrium studies of lysozyme adsorption to Sephadex G-100. (a) Scatchard plot of results for lysozyme in the absence of ligand. (b) Evaluation of the binding constant (K_{AS}) for the lysozyme–glucose interaction by the application of Eq. (20) to results obtained with 8.3 μ M enzyme ($[\bar{A}]$) and a range of glucose concentrations (data taken from [4]).

ciently high concentration of a competing ligand to minimize the interaction of A with immobilized affinity sites, X; or from extrapolation of such analyte distribution data to infinite ligand concentration ($1/[S] \rightarrow 0$). For a univalent analyte the resulting values of $[\bar{A}]$ and $[\bar{A}]$ are then analyzed according to Eqs. (4a) and (4b) in order to determine K_{AX} , $[\bar{X}]$ and K_{AS} (or K_{SX}).

Although the partition of lysozyme into Sephadex is not usually regarded in terms of affinity chromatography, the anomalous gel chromatographic behavior of lysozyme on Sephadex G-100 [33] can be eliminated by including *N*-acetylglucosamine or glucose in the buffer medium [4]. This suppression of lysozyme adsorption to the Sephadex matrix reflects competition between monosaccharide and matrix affinity sites for the single active site of the enzyme—the situation depicted schematically in Fig. 1a.

Because the theory of quantitative affinity chromatography was being expressed in terms of column parameters [4], the concentration distribution of analyte in those partition equilibrium studies of the lysozyme–Sephadex–glucose system were used to evaluate parameters such as \bar{V}_A (the elution volume corresponding to $[\bar{A}]$) and V_A^* , the elution volume of enzyme in the absence of matrix interaction (the counterpart of $[\bar{A}]$). The value of 10.62 ml for V_A^* [4] is reinstated to allow direct interpretation of those partition equilibrium studies in terms of Eqs. (4a) and (4b).

Results obtained with slurries of Sephadex G-100 (0.4 g) in 12 ml acetate-chloride buffer (pH 5.4, I 0.1) containing 0.35–3.35 g lysozyme are presented in Fig. 8a, which signifies a binding constant (K_{AX}) of 1.2×10^6 M⁻¹ for the interaction of enzyme with matrix affinity sites present at an effective total concentration $[\bar{X}]$ of 0.99 μ M. Because the

second series of experiments entailed measurement of the lysozyme distribution in reaction mixtures with a fixed enzyme concentration ($[\bar{A}] = 8.3 \mu\text{M}$) and a range of glucose concentrations, the results are analyzed (Fig. 8b) in accordance with the counterpart of Eq. (15), namely:

$$\frac{([\bar{A}]/[\bar{A}])_0 - ([\bar{A}]/[\bar{A}])_s}{([\bar{A}]/[\bar{A}])_s - 1} = \frac{K_{AS}[S]}{(1 + K_{AX}[\bar{A}]_s)} \quad (20)$$

in which $[\bar{A}]$ ranged between 7.5 and 8.1 μM (mean 7.8 μM). Combination of the slope (3.08 M^{-1}) with the mean value of 10.4 for $(1 + K_{AX}[\bar{A}]_s)$ signifies a binding constant of 32 M^{-1} for the lysozyme–glucose interaction.

A disadvantage of these simple partition experiments is the need for precise control over the amount of affinity matrix added to each reaction mixture. Meeting this requirement posed no great difficulty in the above study [4] because of the availability of the affinity matrix (Sephadex G-100) as a dry powder. However, it can be difficult to accomplish in situations where the affinity matrix needs to be dispensed in the form of a concentrated slurry [6].

The presence of identical amounts of affinity matrix in all reaction mixtures can sometimes be ensured by switching to a recycling procedure (Fig. 9a) in which the liquid phase from a stirred slurry of affinity matrix passes through an analyte-monitoring device before its return to the slurry [5,34]. After equilibration of the slurry with buffer, the addition of an aliquot of stock analyte solution gives rise to a progressive change in the monitored analyte concentration in the liquid phase until a time-independent (equilibrium) value is attained (Fig. 9b, upper trace). Combination of that value of $[\bar{A}]$ with the total analyte concentration deduced from the amount of analyte added then yields one $\{([\bar{A}] - [\bar{A}]), [\bar{A}]\}$ combination. Further additions of stock analyte solution can then be made to generate the whole data set for characterizing the analyte–matrix interaction in terms of K_{AX} and $[\bar{X}]$. Successive aliquots of a stock solution of competing ligand (S) can then be added to provide results for the calculation of K_{AS} or K_{SX} , the equilibrium constant for the competing interaction (Fig. 9b, lower trace).

As noted above the advantage of this recycling procedure is that the amount of affinity matrix is invariant for the whole series of reaction mixtures. However, because the total concentration of matrix sites $[\bar{X}]$ necessarily decreases because of the increase in V_A^* with each addition of analyte (or ligand), allowance needs to be made for this dilution factor. On the grounds that $V_A^*[\bar{X}] = (V_A^*)_0[\bar{X}]_0$, results can be related to the initial matrix-site concentration $[\bar{X}]_0$ by means of the volume ratio $V_A^*/(V_A^*)_0$, where the accessible volume at any stage of the stepwise titration (V_A^*) is greater than its initial value, $(V_A^*)_0$, by the product of the number of aliquots (n) with volume δV that have been added to the slurry:

$$V_A^* = (V_A^*)_0 + n\delta V.$$

Application of the recycling partition procedure is illustrated by a study of the effect of high affinity heparin on

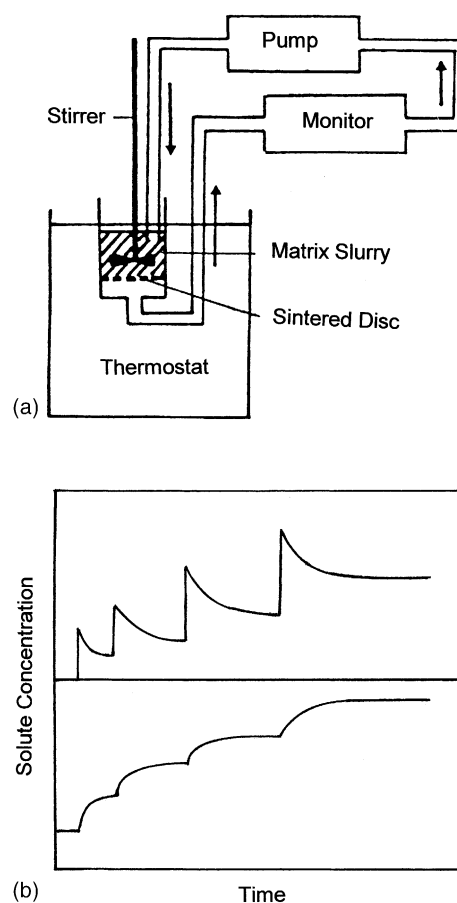


Fig. 9. Studies of ligand binding by the recycling partition procedure [5,34]. (a) Schematic representation of the assembly. (b) Form of the time dependence of monitor response resulting from the stepwise addition of aliquots of analyte (upper trace) and competing ligand (lower trace) to the stirred slurry.

the interaction between antithrombin (a univalent analyte) and heparin-Sepharose [34]. The results of recycling experiments (pH 7.4, 25 °C) involving progressive supplementation of a heparin-Sepharose slurry with antithrombin are summarized in Fig. 10a, which yields a binding constant (K_{AX}) of $6.8 \times 10^6 \text{ M}^{-1}$ for the interaction of antithrombin with immobilized affinity sites, present initially at an effective total concentration $([\bar{X}]_0)$ of 2.2 μM .

Because the competition data had been obtained by successive additions of ligand (high-affinity heparin) to the antithrombin-supplemented slurry, the constitutive equilibrium constant for the analyte–matrix interaction, \bar{K}_{AX} (see Fig. 4), was calculated for each step from the expression:

$$\bar{K}_{AX} = \frac{[\bar{A}] - [\bar{A}]}{[\bar{A}]\{ (V_A^*/(V_A^*)_0)[\bar{X}]_0 - [\bar{A}] + [\bar{A}] \}} \quad (21)$$

In order to determine K_{AS} by the method adopted in Fig. 4b, account must be taken of the fact that the free heparin concentration, $[S]$, differs from its total concentration, $[\bar{S}]$, which is the parameter directly available to the experimenter. The abscissa employed in the analysis of the current results

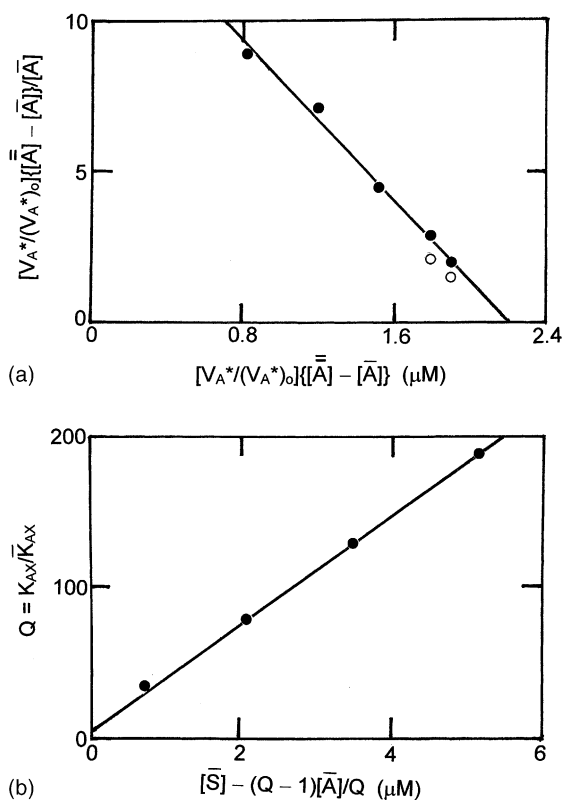


Fig. 10. Characterization of the interaction between high-affinity heparin (S) and antithrombin (A) by recycling partition equilibrium studies (pH 7.4, 25 °C) with heparin-Sepharose as the affinity matrix. (a) Scatchard plot for the evaluation of K_{AX} from data for antithrombin alone. (b) Determination of K_{AS} by the application of Eq. (21) to \bar{K}_{AX} values for heparin–antithrombin mixtures (data taken from [34]).

(Fig. 10) reflects the relationship [27]:

$$[S] = [\bar{S}] - \frac{(Q-1)f[\bar{A}]}{Q}; \quad Q = \frac{K_{AX}}{\bar{K}_{AX}} \quad (22)$$

for situations where K_{AS} is the binding constant for the competing interaction: a binding constant of $3.4 \times 10^7 \text{ M}^{-1}$ is obtained from the slope of Fig. 10b. The corresponding analysis of systems in which K_{SX} describes the competing interaction is slightly more complicated because of the distribution of total ligand concentration across both phases (as S and SX). Specifically, results for that competitive situation need to be analyzed in terms of the expression:

$$(Q-1)K_{AX}[\bar{A}]^{1/f} = K_{SX}\{K_{AX}[\bar{A}]^{1/f}[\bar{S}] - (Q-1)([\bar{A}]^{1/f} - [\bar{A}]^{1/f})\} \quad (23)$$

which signifies determination of K_{SX} as the slope of the dependence of $(Q-1)K_{AX}[\bar{A}]^{1/f}$ upon $\{K_{AX}[\bar{A}]^{1/f}[\bar{S}] - (Q-1)([\bar{A}]^{1/f} - [\bar{A}]^{1/f})\}$ [27,35].

3.4. Radioimmunoassay and enzyme-linked immunosorbent assay techniques

The quantification of immunochemical reactions has posed problems because of the strength of antigen–antibody

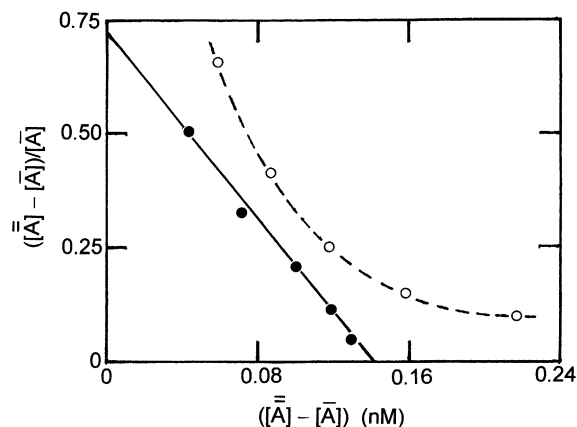


Fig. 11. Scatchard plots inferred from measurements of radioactivity associated with the bead (○) and the liquid phase (●) in a commercial solid-phase radioimmunoassay (T3 RIAbead) for triiodothyronine (data taken from [8]).

interactions. In principle, expressions such as Eqs. (4a) and (4b) [or Eq. (7)] and Eq. (22) could be used for the analysis of solid-phase immunoassays (radioimmunoassay or ELISA). However, difficulties arise because $[\bar{X}]$ is so small in comparison with $[\bar{A}]$ that $[\bar{A}]$ becomes indistinguishable from the total analyte (antibody) concentration. On the grounds that $([\bar{A}] - [\bar{A}])$ cannot therefore be deduced from the extent of analyte depletion in the liquid phase, procedures need to be devised for direct measurement of the concentration of immobilized antibody–antigen complex. This requirement is met in solid-phase immunoassays by removal of antibody from the liquid phase in order that the concentration of complexed antibody can be monitored by radioactivity measurements on the solid phase (radioimmunoassay) or by means of an enzyme conjugated to the second antibody directed against the fixed (Fc) region of the first enzyme-linked immunosorbent assay (ELISA).¹

Inasmuch as the measurement of equilibrium concentrations by isolation of the complex from reaction mixtures contravenes the basic tenets of thermodynamics, this facet of solid-phase immunoassays is clearly a cause for concern. A commonly used approach has entailed the use of cold buffer for the washing steps in an attempt to decrease the rate of complex dissociation. However, it is better to maintain the equilibration temperature but vary the isolation regimen to establish independence of the result upon factors such as the number and volume of washing steps [8,9]. In that regard a situation involving an inadequate washing regimen was encountered [8] in a commercial radioimmunoassay (T3 RIAbead) for triiodothyronine (Fig. 11). These solid-phase

¹ A similar situation is encountered in the use of microaffinity chromatography for detecting protein–protein interactions [36]. However, there is no theoretical basis for the assertion that the dissociation constant ($1/K_{AX}$) may be estimated as one-twentieth of the minimum concentration of immobilized ligand ($[\bar{X}]$) required for observable retention of analyte by the affinity matrix.

immunoassays were conducted in accordance with the recommended instructions, except that the radioactivity of the liquid phase at equilibrium was measured as well as that associated with the washed bead. Whereas the curvilinear form of the Scatchard plot inferred from radioactivity measurements on the washed bead (○) seemingly signifies heterogeneity of the immobilized antibody sites, it actually reflects incomplete removal of unreacted antigen from the bead—a deficiency of the recommended procedure that is revealed by the Scatchard data based on the equilibrium distribution of radioactivity between the two phases (●).

The fact that $[\bar{X}]$ is so small compared with the total concentration of antibody (analyte) in ELISA procedures simplifies matters by justifying the substitution of $[\bar{A}]$ for $[\bar{A}]$ in quantitative expressions. Furthermore, this simplifying situation ($[\bar{X}] \ll f[\bar{A}]$) validates the approximation that antibody interaction with immobilized antigen is restricted to 1:1 complex formation [4,9,35]. A series of experiments with a range of antibody concentrations and a fixed concentration of immobilized antigen sites suffices for the determination of K_{AX} from the expression [9]:

$$\frac{([\bar{A}] - [\bar{A}])_0}{[A]_0} = fK_{AX}[\bar{X}] - fK_{AX}([\bar{A}] - [\bar{A}])_0 \quad (24)$$

where the zero subscript denotes a measurement made in the absence of competing antigen. As noted above, $[\bar{A}]_0$ is an acceptable approximation of $[\bar{A}]_0$ in the ordinate parameter of the Scatchard plot. A second series of experiments is then conducted with constant $[\bar{A}]$ and $[\bar{X}]$ but a range of concentrations of soluble antigen, $[S]$. The ratio of the concentration of matrix-bound antibody in the absence of S to that in its presence, $([\bar{A}] - [\bar{A}])_S$, is given by [9]:

$$\frac{([\bar{A}] - [\bar{A}])_0}{([\bar{A}] - [\bar{A}])_S} = 1 + \frac{K_{AS}[S]}{1 + fK_{AX}[\bar{A}]} \approx 1 + \frac{K_{AS}[S]}{1 + fK_{AX}[\bar{A}]} \quad (25)$$

The linear dependence of the ratio of bound antibody concentrations upon $[S]$ thus defines the magnitude of $K_{AS}/(1 + fK_{AX}[\bar{A}])$; and hence, by incorporation of the K_{AX} value from the first series, the binding constant K_{AS} for the interaction of soluble antigen with f equivalent and independent sites on the antibody.

Application of this procedure to solid-phase immunoassay data on the interaction between paraquat and a monoclonal antibody (IgG) elicited in response to this univalent antigen is summarized in Fig. 12, which refers to results with paraquat immobilized on the surface of ELISA plates [9]. Concentrations of bound antibody, $([\bar{A}] - [\bar{A}])_0$ are expressed in terms of absorbances that reflect catalysis by horseradish peroxidase conjugated to the anti-immunoglobulin antibody used for quantifying bound antibody concentration. An intrinsic binding constant ($f = 2$) with immobilized paraquat is obtained from the slope ($-2K_{AX}$) of the Scatchard plot of results in the absence

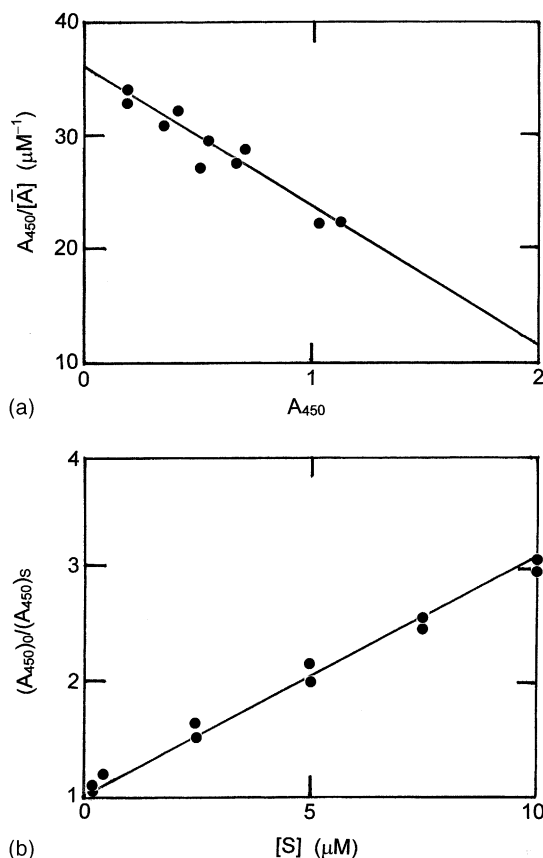


Fig. 12. Quantitative characterization of the interaction between paraquat and an elicited monoclonal antibody by ELISA. (a) Analysis of results for the monoclonal IgG in the absence of antigen according to Eq. (24) with $([\bar{A}] - [\bar{A}])_0$ measured by means of horseradish peroxidase attached to the anti-Fc antibody. (b) Evaluation of the IgG-paraquat binding constant by the application of Eq. (25) to results obtained in the presence of 24 nM antibody and a range of paraquat concentrations (data taken from [9]).

of competing antigen (Fig. 12a). Its combination with the slope, $K_{AS}/(1 + 2K_{AX}[\bar{A}])$, of the data for mixtures containing 24 nM IgG ($[\bar{A}]$) and 0.05–10 μM paraquat (Fig. 12b) yields a K of $2.7 \times 10^5 \text{ M}^{-1}$ for the interaction between unmodified paraquat and its elicited monoclonal antibody [9].

3.5. Biosensor technology

Although solid-phase radioimmunoassay and ELISA techniques continue to be used widely for the characterization of immunochemical interactions, they will presumably be replaced gradually by biosensor methods, which have the advantage of monitoring the concentration of bound analyte, $([\bar{A}] - [\bar{A}])$, in an unperturbed equilibrium mixture of analyte and immobilized affinity ligand. Equilibrium measurements of analyte binding in the BIAcore [37] and BIOS-1 [38] instruments are analogous to frontal affinity chromatography. Thus, a solution of partitioning analyte flows across the affinity matrix, located on the base of a capillary microchannel, until the concentration of analyte in the liquid phase attains its injected value (Fig. 13a).

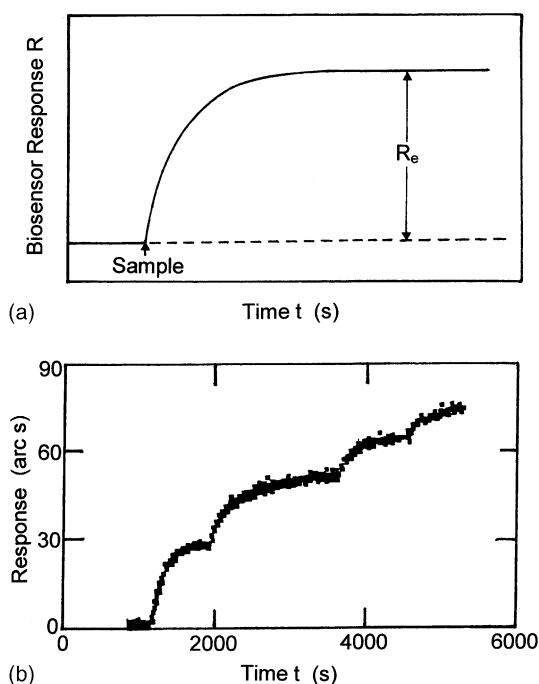


Fig. 13. Thermodynamic studies of ligand binding by biosensor technology. (a) Schematic representation of the time dependence of biosensor response in either a microfluidics-based (BIAcore) or cuvette-based (IASys) instrument: R_e denotes the equilibrium response. (b) Investigation of the interaction between apocarboxypeptidase A and a specific monoclonal antibody by stepwise titration in an IASys cuvette with immobilized antibody on the sensor surface (data taken from [41]).

On the other hand, the characterization of analyte interactions by means of the IASys [39] and IBIS [40] instruments is more akin to partition equilibrium studies in that complex formation on the sensor surface occurs at the expense of the analyte concentration in the liquid phase. The time course of biosensor response retains the form shown in Fig. 13a, but the time-independent response (R_e) refers to the concentration of immobilized AX complex in equilibrium with a liquid-phase analyte concentration ($[\bar{A}] - [AX]$) rather than $[\bar{A}]$ (the initial value). This necessity to take into account the disparity between $[\bar{A}]$ and $[\bar{A}] = [\bar{A}] - [AX]$ tends to be regarded as a disadvantage of cuvette-based biosensors. However, that disadvantage is offset by compatibility of the instrumental design with the conduct of stepwise titrations [41] (Fig. 13b). Indeed, this feature has been deemed sufficiently advantageous to warrant adaptation of the BIAcore-X flow-cell instrument into a recycling equivalent of a cuvette-based system [42].

Thermodynamic analysis of measurements obtained with a flow-cell-based biosensor for a univalent analyte is based on the expression:

$$\frac{R_e}{[\bar{A}]} = \left\{ \frac{K_{AX}}{1 + K_{AS}[S]} \right\} R_m - \left\{ \frac{K_{AX}}{1 + K_{AS}[S]} \right\} R_e \quad (26)$$

in which R_e and R_m are the respective responses corresponding to $([\bar{A}] - [\bar{A}])$ and $[\bar{X}]$ in Eq. (4a). Such substitution of

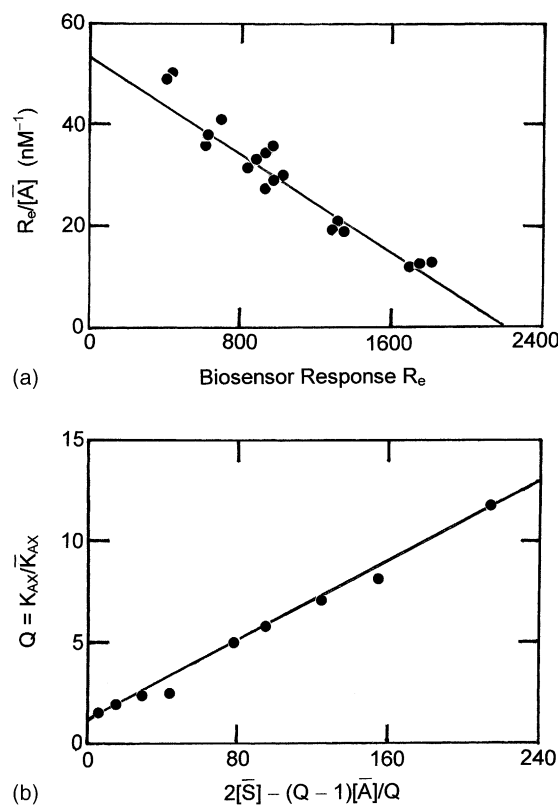


Fig. 14. Characterization of the interaction between dimeric interleukin-6 (S) and the soluble form of its biospecific receptor (A) by means of a BIAcore biosensor with immobilized cytokine as X. (a) Evaluation of K_{AX} by the application of Eq. (26). (b) Determination of K_{AS} for the interaction between receptor and interleukin-6 in solution (data taken from [10]).

responses for concentrations of bound analyte has been justified experimentally by demonstration of their direct proportionality in optical biosensors based on surface plasmon resonance [43] and resonant mirror [39] technologies. Application of this expression to BIAcore results obtained [10] for the interaction of the soluble form of interleukin-6 receptor with interleukin-6 immobilized on a carboxymethyl dextran sensor chip is shown in Fig. 14a, which signifies a value of $2.4 \times 10^7 \text{ M}^{-1}$ for K_{AX} and a maximal matrix capacity for analyte corresponding to 2200 response units (R_m). In order to obtain an equilibrium constant for the cytokine-receptor interaction in solution, receptor solutions supplemented with interleukin-6 were flowed across the same sensor chip to obtain the constitutive analyte–matrix binding constant, $\bar{K}_{AX} = K_{AX}/(1 + K_{AS}[S])$. Because the ligand concentration available to the experimenter is $[\bar{S}]$, the free interleukin-6 concentration pertinent to each K value needs to be determined by a counterpart of Eq. (22) that takes into account the bivalence of the dimeric interleukin-6. The consequent evaluation of K_{AS} is shown in Fig. 14b, the slope of which yields a binding constant of $4.8 \times 10^7 \text{ M}^{-1}$ for the interaction between receptor and unmodified interleukin-6 [10].

4. Extension of the approach to high-performance affinity chromatography

The use of high-performance affinity chromatography as a means of determining binding constants for protein–drug interactions is a rapidly growing field (reviewed in [15]). A protein, frequently serum albumin, is immobilized on a rigid chromatographic matrix such as modified silica to allow monitoring of a protein–drug interaction by the extent to which elution of the drug is retarded. Competitive binding studies with a range of other drugs are then conducted in order to compare binding strengths on the basis of the decreased extent of retardation of the drug whose interaction is being monitored. Although such studies are encompassed by the situation depicted in Fig. 1b, their analytical treatment has been developed independently of the theoretical expressions already available in the context of conventional quantitative affinity chromatography. The purpose of this section is to reconsider the analysis of high-performance affinity chromatography results in the light of present theory; and thereby to correlate the quantitative treatments.

4.1. Drug interaction with a single class of immobilized affinity sites

The experimental parameter derived from high-performance affinity chromatography is the retention factor for analyte, which is defined in present terminology as:

$$\bar{k}_A = \frac{\bar{t}_A - t_A^*}{t_A^*} = \frac{\bar{V}_A}{V_A^*} - 1 \quad (27)$$

where \bar{t}_A and t_A^* are the respective retention times corresponding to \bar{V}_A and V_A^* . From Eq. (6b) it follows that frontal chromatographic data for a univalent analyte may be analyzed quantitatively in terms of the expression:

$$\bar{k}_A[\bar{A}] = (\bar{A}) - [\bar{A}] = \frac{\{K_{AX}/(1 + K_{SX}[S])\}[\bar{X}][\bar{A}]}{1 + \{K_{AX}/(1 + K_{SX}[S])\}[\bar{A}]} \quad (28)$$

which should suffice to describe the interaction of a small drug with equivalent and independent sites on the immobilized serum albumin.

The above situation has been encountered in an investigation [44] that reports retention factors obtained by zonal chromatography of *R*-ibuprofen on an albumin affinity column pre-equilibrated with a range of concentrations of the same drug. Although determined by zonal elution, the value of \bar{k}_A effectively refers to the retention factor in a frontal chromatography experiment with the applied drug concentration equal to the pre-equilibrating concentration ($[\bar{A}]$) of *R*-ibuprofen. Those results for *R*-ibuprofen (Table 1 of [44]) are therefore analyzed (Fig. 15a) in terms of Eq. (28) with $[S] = 0$. The binding constant (K_{AX}) of $5.8 \times 10^5 \text{ M}^{-1}$ and an effective column capacity ($[\bar{X}]$) of $121 \mu\text{M}$ were also

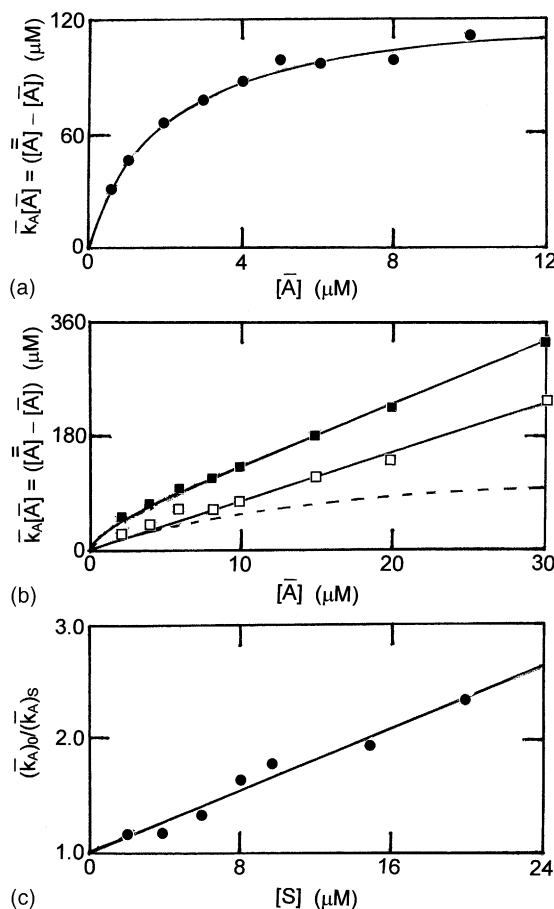


Fig. 15. Studies of albumin–drug interactions by high-performance affinity chromatography on a column with immobilized albumin as affinity ligand. (a) Dependence of the concentration of bound *R*-ibuprofen upon its concentration in the liquid phase. (b) Corresponding dependence for *S*-ibuprofen (■), together with those for its interaction with sites accessible to the *R*-isomer (---) and the residual binding requiring quantitative description (□). (c) Characterization of the interaction of *S*-ibuprofen that competes with the *R*-isomer for immobilized albumin sites by zonal chromatography of *R*-ibuprofen in the presence of *S*-ibuprofen [Eq. (31)] (data taken from [44]).

obtained by using the double-reciprocal linear transform of Eq. (28) [44].

4.2. Allowance for heterogeneity of immobilized affinity sites

Because serum albumin is often the immobilized ligand, consideration needs to be given to the possibility that analyte (drug) binds to more than one class of binding sites. For equivalent and independent binding of analyte to two classes of site on immobilized ligand the counterpart of Eq. (28) becomes:

$$\bar{k}_A[\bar{A}] = \frac{K_1[\bar{X}][\bar{A}]}{1 + K_1[\bar{A}]} + \frac{K_2(q/p)[\bar{X}][\bar{A}]}{1 + K_2[\bar{A}]} \quad (29)$$

where K_1 and K_2 denote the respective intrinsic binding constants [18] for the interactions of analyte with p and q

sites of each class on the immobilized albumin. This is essentially the approach adopted in high-performance affinity chromatography [15,44], except that the (q/p) factor was omitted.

The counterpart of Fig. 15a deduced from the \bar{k}_A values for *S*-ibuprofen on an albumin column pre-equilibrated with the same isomer (Table 2 of [44]) is shown (■) in Fig. 15b, which clearly deviates from the simple rectangular hyperbolic dependence observed for *R*-ibuprofen (Fig. 15a). Furthermore, the concentration of drug bound by the column ($\bar{k}[\bar{A}]$) exceeds that for the *R*-isomer—an observation that signifies *S*-ibuprofen interaction with sites additional to those accessed by *R*-ibuprofen. Before any attempt is made to analyze the form of Fig. 15b it is advantageous to glean more information from the competitive binding studies reported in [44].

4.3. Determination of binding constants from competitive binding experiments

As well as containing the retention times already considered, Tables 1 and 2 of [44] also include those for zones of one ibuprofen isomer (A) on an albumin column pre-equilibrated with a range of concentrations [S], of the other. This second series of experiments thus conforms with the standard protocol for the determination of binding constants by zonal affinity chromatography [3]. For situations in which the pre-equilibration drug (S) competes for all immobilized affinity sites accessed by the analyte (A), the results require analysis in terms of the expression:

$$(\bar{k}_A)_S = \frac{K_{AX}[\bar{X}]}{1 + K_{SX}[S]} \quad (30)$$

which is the counterpart of Eq. (17). Upon noting that the retention factor measured in the absence of competing ligand ($(\bar{k}_A)_0$), affords the magnitude of $K_{AX}[\bar{X}]$, Eq. (30) may also be written as:

$$\frac{(\bar{k}_A)_0}{(\bar{k}_A)_S} = 1 + K_{SX}[S] \quad (31)$$

This completely competitive situation is thus recognized by a linear dependence of \bar{k}_A^0/\bar{k}_A upon [S] that also defines the magnitude of K_{SX} . A similar dependence applies to systems in which analyte only binds to one of the classes of site accessible to the pre-equilibrating ligand [45,46]. However, the value of K_{SX} obtained by this means refers only to the interaction of the second drug with the class of sites to which A binds.

In the context of Fig. 15, the greater capacity exhibited by the albumin affinity column for *S*-ibuprofen signifies that the application of this approach to $(\bar{k}_A)_S$ values for *R*-ibuprofen in the presence of the other isomer affords access to K_{SX} for the interaction of *S*-ibuprofen with the class of immobilized sites to which the *R*-isomer binds (Fig. 15c). Knowledge of this binding constant ($6.7 \times 10^4 \text{ M}^{-1}$) allows construction of the binding curve for occupancy of this class of matrix

sites (---, Fig. 15b); and hence, by difference, delineation of binding data for the additional uptake of *S*-ibuprofen by the albumin affinity column (□, Fig. 15b). In that regard, the essential linearity of the dependence precludes any quantitative assessment of this second phenomenon in terms of ligand binding.

4.4. Binding parameters for the drug-albumin interaction in solution

Although K_{AX} and K_{SX} have been considered to describe the respective interactions of drugs with serum albumin, they actually refer to drug interactions with a chemically modified (immobilized) derivative of albumin. This potential deficiency of the high-performance affinity chromatography approach has been recognized in the sense that attention has been drawn to the agreement between values of K_{AX} or K_{SX} and their counterparts from studies of the corresponding albumin–drug interactions in solution [15,47,48]. The fact that no attempt seems to have been made to characterize the solution-phase interaction by high-performance affinity chromatography is surprising inasmuch as quantitative affinity chromatography was devised for that specific purpose [4,5,13,14,27,28]. The following procedure should serve to rectify that current deficiency of high-performance affinity chromatography for the characterization of albumin–drug interactions.

Whereas competitive binding studies in high-performance affinity chromatography have previously involved a second reactant with affinity for the immobilized ligand (the situation represented in Fig. 1b), the use of serum albumin as the second reactant has the potential to provide quantitative information on the competing interaction in the solution phase (the scheme depicted in Fig. 1a). Inclusion of albumin in the applied mixture decreases the measured retention factor for drug, $(\bar{k}_A)_S$, because of the decreased concentration of free drug that is available for reaction with immobilized albumin sites X. Specifically, the measurement of $(\bar{k}_A)_S$ by frontal chromatography of a mixture of drug (A) and albumin (S) with composition ($[\bar{A}]$, $[\bar{S}]$) allows the free drug concentration, [A], to be calculated from the expression:

$$(k_A)_S[\bar{A}] = \frac{K_{AX}[\bar{X}]}{1 + K_{AX}[A]} \quad (32)$$

provided that K_{AX} and the effective total concentration of immobilized albumin sites ($[X]$) have already been determined from chromatographic experiments on drug alone. Alternatively, the dependence of $(\bar{k}_A)_0$ upon drug concentration in the absence of competing albumin may be used as a calibration plot to define the free analyte concentration in the solution phase on the basis of $(\bar{k}_A)_S$ for a reaction mixture with total drug concentration $[\bar{A}]$. Such a procedure has been illustrated in the biosensor variant of quantitative affinity chromatography [10].

Knowledge of [A] for a solution-phase mixture with composition ($[\bar{A}]$, $[\bar{S}]$) allows calculation of the conventional

binding function for drug, r , as:

$$r = \frac{[\bar{A}] - [A]}{[\bar{S}]} \quad (33)$$

A series of frontal chromatography experiments with a fixed albumin concentration ($[\bar{S}]$) and a range of drug concentrations ($[\bar{A}]$) should thus generate a binding curve (r versus $[A]$) equivalent to that which could have been obtained by equilibrium dialysis. Evaluation of binding parameters by curve-fitting the binding data to the expression:

$$r = \frac{pK_1[A]}{1 + K_1[A]} + \frac{qK_2[A]}{1 + K_2[A]} \quad (34)$$

then has the capacity to yield estimates of p , q , K_1 and K_2 that refer unequivocally to the stoichiometries and strengths of the interactions between drug and serum albumin in solution—the information really being sought in high-performance affinity chromatography.

5. Interactions of glycolytic enzymes with muscle myofibrils

In most studies considered so far, the affinity matrix has merely afforded a means of characterizing a biospecific interaction in the liquid phase by quantitative affinity chromatography. In the biological environment, however, there are many naturally occurring phenomena wherein the biphasic distribution of a solute (analyte) between soluble and adsorbed states reflects biospecific complex formation with components embedded in the cellular/subcellular matrix. This section concludes with a demonstration of the manner in which the same theoretical expressions (or adaptations thereof) may be used to advantage for the characterization of these naturally occurring examples of affinity chromatography. The interaction of glycolytic enzymes with the muscle myofibrillar matrix is selected for this purpose.

5.1. Interaction of aldolase with the myofibrillar matrix

Studies of the interaction between aldolase and skeletal muscle myofibrils provided an early example of simple partition equilibrium experiments being used to characterize the biphasic distribution of proteins in terms of quantitative affinity chromatography theory [6]. Those studies were conducted at a stage when there was considerable interest in the concept that a myofibril-bound complex of glycolytic enzymes afforded an efficient means of regulating metabolic flux to meet the continually varying energy requirements of the muscle cell [49,50]. Much of the evidence purported to favor the concept of glycolytic enzyme adsorption to muscle thin filaments had been restricted to qualitative demonstrations of interactions at low ionic strength. The following studies thus represented the first attempt to establish the existence of interactions between glycolytic enzymes and my-

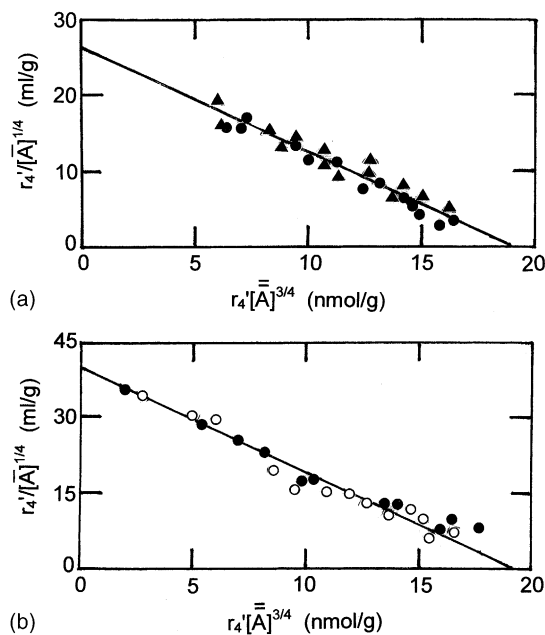


Fig. 16. Multivalent Scatchard analyses [Eq. (33)] of results obtained in partition equilibrium studies of the interactions of glycolytic enzymes with skeletal muscle myofibrils (pH 6.8, I 0.16). (a) Results for aldolase taken from [6] (●) and [7] (▲). (b) Results for glyceraldehyde-3-phosphate dehydrogenase in the absence (○) and presence (●) of aldolase (data taken from [7]).

ofibrils under conditions physiological with respect to ionic strength.

Because there is no means of ascertaining beforehand the magnitude of $[\bar{X}]$, the effective molar concentration of matrix affinity sites for each myofibril–enzyme slurry, the matrix concentration can be expressed initially on a mass-concentration basis, \bar{c}_X . Furthermore, experiments may be considered as ligand-binding studies, whereupon it is appropriate to examine the results in such terms. For an f -valent partitioning solute (analyte) the binding function, r'_f , is defined [7,19] as:

$$r'_f = ([\bar{A}]^{1/f} - [\bar{A}]^{1/f})/\bar{c}_X \quad (35)$$

and the counterpart of the Scatchard expression [Eq. (17)] becomes:

$$\frac{r'_f}{[\bar{A}]^{1/f}} = \frac{K_{AX}}{1/M_X} - fK_{AX}r'_f[\bar{A}]^{(f-1)/f} \quad (36)$$

where $1/M_X$, the counterpart of $[\bar{X}]$, is the matrix capacity (mol/g) for analyte (partitioning solute).

Results [6,7] for the interaction of aldolase with rabbit skeletal muscle myofibrils (pH 6.8, I 0.16) are summarized in Fig. 16a, which is based on a valence of four for this tetrameric enzyme. Analysis of the results in terms of Eq. (33) with $f = 4$ signifies an intrinsic binding constant K_{AX} of $360,000 \text{ M}^{-1}$ and an effective matrix capacity ($1/M_X$) of 76 nmol/g for the aldolase–myofibril interaction (Fig. 16a). These studies thus provide credible evidence for

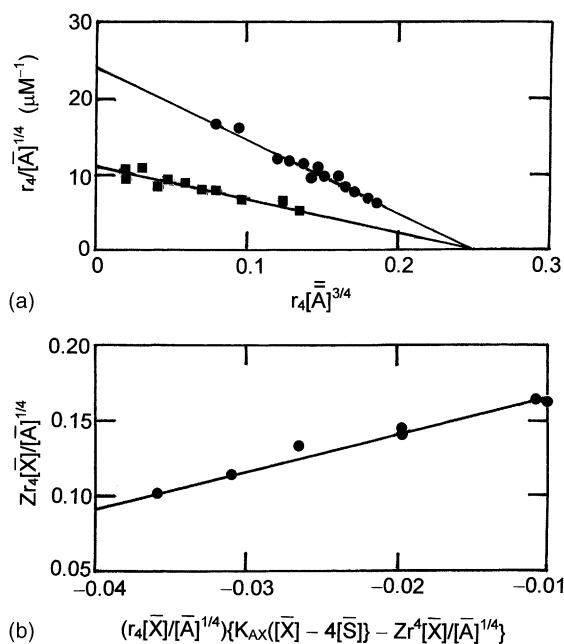


Fig. 17. Partition equilibrium studies of the interactions of glycolytic enzymes with cardiac muscle myofibrils (pH 6.8, I 0.16). (a) Multivalent Scatchard plots of results in separate studies with lactate dehydrogenase (■) and aldolase (●) as analyte. (b) Binding of lactate dehydrogenase (A) in the presence of an equal concentration of aldolase (S), the results being plotted according to Eq. (34) (data taken from [45]).

the binding of aldolase to the myofibrillar matrix as a physiologically significant phenomenon.

5.2. Myofibrillar interactions of other glycolytic enzymes

The demonstration of aldolase interaction with the myofibrillar matrix under conditions physiological with respect to ionic strength was followed by similar evidence [7] of myofibrillar interactions with glyceraldehyde-3-phosphate dehydrogenase, another tetrameric enzyme. Myofibrils exhibit the same capacity but a stronger affinity ($K_{AX} = 510,000 \text{ M}^{-1}$) for this enzyme (○, Fig. 16b). Furthermore, the essentially identical binding characteristics for the interaction between glyceraldehyde-3-phosphate dehydrogenase in the presence of aldolase (●, Fig. 16b) signifies independence of the two binding phenomena.

The binding characteristics of aldolase have also been compared with those of lactate dehydrogenase in studies with myofibrils from bovine cardiac muscle [45], which exhibit the same capacity (76 nmol/g) but a weaker affinity for glycolytic enzymes. Whereas $K_{AX} = 360,000 \text{ M}^{-1}$ for the aldolase interaction with skeletal muscle myofibrils (Fig. 16a), the corresponding value for cardiac muscle myofibrils is only $240,000 \text{ M}^{-1}$ (● in Fig. 17a, where the binding is expressed in terms of the conventional binding function, r_f , by incorporation of the myofibrillar capacity, $1/M_X$). A smaller binding constant ($K_{AX} = 110,000 \text{ M}^{-1}$) describes the interaction of lactate dehydrogenase with these myofibrils (■, Fig. 17a). In contrast with the situation observed in

Fig. 16b for aldolase and glyceraldehyde-3-phosphate dehydrogenase, the myofibrillar interactions of aldolase and lactate dehydrogenase are mutually exclusive (competitive). This is demonstrated in Fig. 17b, which plots results for the binding of lactate dehydrogenase (analyte A) in the presence of an equal concentration of aldolase (competing ligand S) in accordance with the expression for competitive interaction, namely [45]:

$$\frac{Zr_f[\bar{X}]}{[\bar{A}]^{1/f}} = K_{AX}[\bar{X}] + \left(\frac{K_{SX}}{K_{AX}}\right) \left(\frac{r_f[\bar{X}]}{[\bar{A}]^{1/f}}\right) \times \left\{ K_{AX}[\bar{X}] - f[\bar{S}] - \frac{Zr_f[\bar{X}]}{[\bar{A}]^{1/f}} \right\} \quad (37a)$$

$$Z = 1 + fK_{AX}[\bar{A}]^{1/f}[\bar{A}]^{(f-1)/f} \quad (37b)$$

These results clearly conform with the linear dependence predicted by Eq. (34), and the value of $260,000 \text{ M}^{-1}$ for K_{SX} that is obtained from the slope (K_{SX}/K_{AX} with $K_{AX} = 110,000 \text{ M}^{-1}$) essentially duplicates the K_{AX} of $240,000$ that is obtained from Fig. 17a for the aldolase–myofibril interaction. Such evidence of competition between glycolytic enzymes for the same matrix affinity sites clearly questions the concept of glycolysis being effected by a complex attached to the myofibrillar matrix.

5.3. Metabolite-effected desorption of aldolase from myofibrils

The concept of a functional myofibril-bound complex of glycolytic enzymes was dealt a further blow by implications that the active site of aldolase is involved in its myofibrillar interaction. The possibility of active-site involvement in aldolase adsorption was first suggested by close correspondence between the magnitude of K_{AS} deduced for phosphate competition in partition studies and the $1/K_I$ for competitive inhibition of the enzyme-catalyzed cleavage of fructose-1,6-bisphosphate [6]. More substantive evidence was provided subsequently [51] by the demonstration that myofibrils inhibited competitively the hydrolysis of fructose-1,6-bisphosphate by aldolase (Fig. 18a). Furthermore, there was again good agreement between the partition equilibrium (K_{AX}) and enzyme kinetic ($1/K_I$) estimates of the binding constant for the aldolase–myofibril interaction [51]. Any direct involvement of myofibril-bound aldolase in glycolysis is thus precluded. Instead, active-site involvement in the interaction of aldolase with myofibrils signifies the likely release of the enzyme into the cytoplasm in response to increased glycolytic flux.

Additional aldolase desorption from the myofibrillar matrix is effected by the increase in Ca^{2+} concentration that triggers muscle contraction (Fig. 18b). This inhibitory effect of Ca^{2+} on the myofibrillar adsorption of aldolase is demonstrably non-competitive [52]—a finding consistent with Ca^{2+} binding by the troponin component of thin filaments rather than the tropomyosin, to which aldolase binds

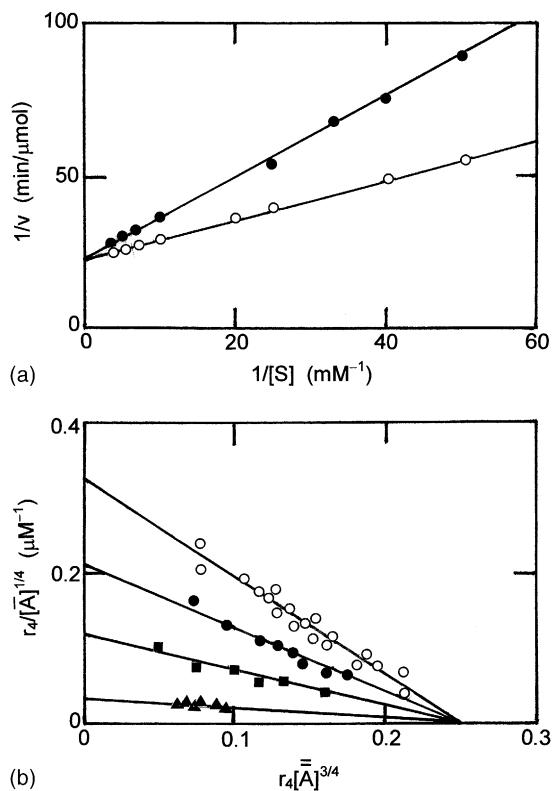


Fig. 18. Effects of metabolites on the interaction between aldolase and skeletal muscle myofibrils. (a) Lineweaver–Burk plots of the kinetics of aldolase-catalyzed cleavage of fructose-1,6-bisphosphate in the absence (○) and presence (●) of myofibrils (2.08 μM) (data taken from [51]). (b) Multivalent Scatchard plots of partition equilibrium results showing the effect of Ca^{2+} concentration on the aldolase–myofibril interaction: (○) zero, (●) 10 μM , (■) 25 μM , (▲) 100 μM Ca^{2+} (data taken from [52]).

[53]. Indeed, these simple partition equilibrium studies sufficed to establish that the 10-fold decrease in constitutive binding constant (\bar{K}_{AX}) for the aldolase–myofibrils interaction reflected attachment of Ca^{2+} to either or both matrix sites for the metal ion [52]. Furthermore, the inferred intrinsic binding constant (K_{SX}) matches closely the measured value for the interaction of Ca^{2+} with the low-affinity sites of troponin C [54], thin filaments [55] and intact muscle [56]. The concept of a myofibril-bound multi-enzyme complex as a facilitator of glycolytic flux [49,50] has clearly lost even more of its appeal as the result of the demonstration of its partial disintegration [51,52] at the very stage when the need to maximize glycolytic flux is greatest.

6. Concluding remarks

Quantitative affinity chromatography is one of the most versatile techniques available for the characterization of ligand binding. It has been used to characterize the binding of small molecules to macromolecules [2–5] as well as reactions involving two macromolecular species [10,34]. Another advantage of affinity chromatography is its ability

to encompass the characterization of interactions with an extremely broad range of equilibrium constants – below 10^3 M^{-1} [4,5] to greater than 10^8 M^{-1} [40].

The fact that there are different methodological approaches to quantitative affinity chromatography allows an experimenter to choose a protocol that is most suited to the particular system under study. There is a choice between elution volume measurements in either zonal or frontal chromatography, as well as between concentration measurements in either the liquid phase or the solid phase in partition equilibrium studies. In situations where amounts of materials are limited, the technique that is most sparing of the reactant in shortest supply can usually be selected without compromising the quality of binding information obtained. In particular, advances in methodology for data capture now allow column chromatographic experiments to be conducted on a micro-scale that was not envisaged at the time of the theoretical developments in quantitative affinity chromatography.

Finally, as illustrated in Section 5, developments in quantitative affinity chromatography over the past 30 years have the potential to improve our approach to understanding ligand-mediated changes in the subcellular distribution of solutes between soluble and particulate states in the physiological environment. Because of its biospecificity, the interaction between solute and particulate receptor may be regarded as a naturally occurring example of affinity chromatography in the cellular environment; and may therefore be studied quantitatively by means of the theoretical expressions developed in the context of quantitative affinity chromatography.

References

- [1] P. Cuatrecasas, C.B. Anfinsen, *Annu. Rev. Biochem.* 40 (1971) 259.
- [2] P. Andrews, B.J. Kitchen, D.J. Winzor, *Biochem. J.* 135 (1973) 897.
- [3] B.M. Dunn, I.M. Chaiken, *Proc. Natl. Acad. Sci. U.S.A.* 71 (1974) 2382.
- [4] L.W. Nichol, A.G. Ogston, D.J. Winzor, W.H. Sawyer, *Biochem. J.* 143 (1974) 435.
- [5] L.W. Nichol, L.D. Ward, D.J. Winzor, *Biochemistry* 20 (1981) 4856.
- [6] M.R. Kuter, C.J. Masters, D.J. Winzor, *Arch. Biochem. Biophys.* 225 (1983) 384.
- [7] S.J. Harris, D.J. Winzor, *Arch. Biochem. Biophys.* 275 (1989) 185.
- [8] P.J. Hogg, D.J. Winzor, *Arch. Biochem. Biophys.* 254 (1987) 92.
- [9] P.J. Hogg, S.C. Johnston, M.R. Bowles, S.M. Pond, D.J. Winzor, *Mol. Immunol.* 24 (1987) 797.
- [10] L.D. Ward, G.J. Howlett, A. Hammacher, J. Weinstock, K. Yasukawa, R.J. Simpson, D.J. Winzor, *Biochemistry* 34 (1995) 2901.
- [11] D.R. Hall, D.J. Winzor, *J. Chromatogr. B* 715 (1998) 163.
- [12] D.J. Winzor, in: P. Matejtschuk (Ed.), *Affinity Separations: A Practical Approach*, IRL Press, Oxford, 1997, p. 39.
- [13] D.J. Winzor, *J. Biochem. Biophys. Methods* 49 (2001) 99.
- [14] D.J. Winzor, in: D.S. Hage (Ed.), *Handbook of Affinity Chromatography*, Marcel Dekker, New York, 2003, in press.
- [15] D.S. Hage, *J. Chromatogr. B* 768 (2002) 300.
- [16] A.J. Muller, P.W. Carr, *J. Chromatogr.* 284 (1984) 33.
- [17] G. Scatchard, *Ann. N. Y. Acad. Sci.* 51 (1949) 660.
- [18] I.M. Klotz, *Arch. Biochem.* 9 (1946) 109.

- [19] P.J. Hogg, D.J. Winzor, *Biochim. Biophys. Acta* 843 (1985) 159.
- [20] D.A. Bergman, D.J. Winzor, *Anal. Biochem.* 153 (1986) 380.
- [21] P.J. Flory, *J. Am. Chem. Soc.* 63 (1941) 3083.
- [22] D.J. Winzor, *Anal. Biochem.* 308 (2002) 409.
- [23] D.J. Winzor, H.A. Scheraga, *Biochemistry* 2 (1963) 1263.
- [24] P.J. Hogg, D.J. Winzor, *Arch. Biochem. Biophys.* 234 (1984) 55.
- [25] P. Kyprianou, R.J. Yon, *Biochem. J.* 207 (1982) 549.
- [26] L.W. Nichol, W.H. Sawyer, D.J. Winzor, *Biochem. J.* 112 (1969) 259.
- [27] D.J. Winzor, C.M. Jackson, in: T. Kline (Ed.), *Handbook of Affinity Chromatography*, Marcel Dekker, New York, 1993, p. 253.
- [28] D.J. Winzor, in: P.D.G. Dean, W.S. Johnson, F.A. Middle (Eds.), *Affinity Chromatography: A Practical Approach*, IRL Press, Oxford, 1985, p. 149.
- [29] E. Brekkan, A. Lundqvist, P. Lundahl, *Biochemistry* 35 (1996) 12141.
- [30] H.E. Swaisgood, I.M. Chaiken, in: I.M. Chaiken (Ed.), *Analytical Affinity Chromatography*, CRC Press, Boca Raton, FL, 1987, p. 65.
- [31] B.M. Dunn, J. Danner-Rabovsky, J. Cambias, in: I.M. Chaiken, M. Wilchek, I. Parikh (Eds.), *Affinity Chromatography and Biological Recognition*, Academic Press, New York, 1983, p. 93.
- [32] R.I. Brinkworth, C.J. Masters, D.J. Winzor, *Biochem. J.* 151 (1975) 631.
- [33] J.R. Whitaker, *Anal. Chem.* 35 (1963) 1950.
- [34] P.J. Hogg, C.M. Jackson, D.J. Winzor, *Anal. Biochem.* 192 (1991) 303.
- [35] N.L. Kalinin, L.D. Ward, D.J. Winzor, *Anal. Biochem.* 228 (1995) 238.
- [36] T. Formosa, J. Barry, B.M. Alberts, J. Greenblatt, *Methods Enzymol.* 208 (1991) 24.
- [37] R. Karlsson, A. Michäelson, L. Mattson, *J. Immunol. Methods* 145 (1991) 229.
- [38] A. Bernard, H.R. Bossard, *Eur. J. Biochem.* 230 (1991) 416.
- [39] P.R. Edwards, A. Gill, D.V. Pollard-Knight, M. Hoare, P.E. Buckle, P.J. Lowe, R.J. Leatherbarrow, *Anal. Biochem.* 231 (1995) 210.
- [40] N.J. de Mol, E. Plomp, M.J.E. Fischer, R. Ruijtenbeek, *Anal. Biochem.* 279 (2000) 61.
- [41] D.R. Hall, D.J. Winzor, *Anal. Biochem.* 244 (1997) 152.
- [42] P. Schuck, D.B. Millar, A. Korrt, *Anal. Biochem.* 265 (1998) 79.
- [43] E. Stenberg, B. Persson, H. Roos, C. Urbaniczky, *J. Colloid Interface Sci.* 143 (1991) 513.
- [44] D.S. Hage, T.A.G. Noctor, I.W. Wainer, *J. Chromatogr. A* 693 (1995) 23.
- [45] S.J. Harris, D.J. Winzor, *Anal. Biochem.* 169 (1988) 319.
- [46] A.M. Brocklebank, W.H. Sawyer, J.S. Wiley, D.J. Winzor, *Anal. Biochem.* 213 (1993) 104.
- [47] B. Loun, D.S. Hage, *J. Chromatogr.* 579 (1992) 225.
- [48] B. Loun, D.S. Hage, *Anal. Chem.* 71 (1994) 3814.
- [49] B.I. Kurganov, N.P. Sugrobova, L.S. Mil'man, *J. Theor. Biol.* 116 (1985) 509.
- [50] F.M. Clarke, P. Stephan, D.J. Morton, J. Weideman, in: R. Beitner (Ed.), *Regulation of Carbohydrate Metabolism*, CRC Press, Boca Raton, FL, 1985, p. 1.
- [51] S.J. Harris, D.J. Winzor, *Biochim. Biophys. Acta* 911 (1987) 121.
- [52] S.J. Harris, D.J. Winzor, *Biochim. Biophys. Acta* 999 (1989) 95.
- [53] F.M. Clarke, P. Stephan, G. Huxham, D. Hamilton, D.J. Morton, *Eur. J. Biochem.* 138 (1984) 643.
- [54] J.D. Potter, J. Gergely, *J. Biol. Chem.* 250 (1975) 4628.
- [55] H.G. Zot, S. Iida, J.D. Potter, *Chem. Scripta* 21 (1983) 133.
- [56] H.G. Zot, J.D. Potter, *J. Biol. Chem.* 257 (1982) 7678.